Deregulation of Protein Phosphatase 2A and Hyperphosphorylation of τ Protein Following Onset of Diabetes in NOD Mice

Marie-Amélie Papon,[1] Noura B. El Khoury,[1,2] François Marcouiller,[1,2] Carl Julien,[1,2] Françoise Morin,[1] Alexis Bretteville,[1,2] Franck R. Petry,[1,2] Simon Gaudreau,[3] Abdelaziz Amrani,[3] Paul M. Mathews,[4,5] Sébastien S. Hébert,[1,2] and Emmanuel Planel[1,2]

The histopathological hallmarks of Alzheimer disease (AD) include intraneuronal neurofibrillary tangles composed of abnormally hyperphosphorylated τ protein. Insulin dysfunction might influence AD pathology, as population-based and cohort studies have detected higher AD incidence rates in diabetic patients. But how diabetes affects τ pathology is not fully understood. In this study, we investigated the impact of insulin dysfunction on τ phosphorylation in a genetic model of spontaneous type 1 diabetes: the nonobese diabetic (NOD) mouse. Brains of young and adult female NOD mice were examined, but young NOD mice did not display τ hyperphosphorylation. τ phosphorylation at τ-1 and pS422 epitopes was slightly increased in nondiabetic adult NOD mice. At the onset of diabetes, τ was hyperphosphorylated at the τ-1, AT8, CP13, pS262, and pS422. A subpopulation of diabetic NOD mice became hypothermic, and τ hyperphosphorylation further extended to paired helical filament-1 and TG3 epitopes. Furthermore, elevated τ phosphorylation correlated with an inhibition of protein phosphatase 2A (PP2A) activity. Our data indicate that insulin dysfunction in NOD mice leads to AD-like τ hyperphosphorylation in the brain, with molecular mechanisms likely involving a deregulation of PP2A. This model may be a useful tool to address further mechanistic association between insulin dysfunction and AD pathology. ***Diabetes*** **62:609–617, 2013**

The two histopathological hallmarks of Alzheimer disease (AD) are senile plaques composed of extracellular aggregates of the β-amyloid (Aβ) peptides and intraneuronal neurofibrillary tangles (NFTs), composed of abnormally hyperphosphorylated τ protein assembled into paired helical filaments (PHFs). τ is a microtubule-associated protein that is abundant in the central nervous system and expressed mainly in axons. τ hyperphosphorylation can induce its aggregation in vitro and is thought to induce NFT formation in the brain (1). Understanding the mechanism, progression, and consequences of τ pathology is important because its extent shows a strong relationship to dementia in AD and to memory loss in normal aging and mild cognitive impairment (2).

From the [1]Centre Hospitalier de l'Université Laval, Axe Neurosciences, Québec, Canada; the [2]Département de Psychiatrie et Neurosciences, Faculté de Médecine, Université Laval, Québec, Canada; the [3]Département de Pédiatrie, Université de Sherbrooke, Sherbrooke, Québec, Canada; [4]The Nathan Kline Institute for Psychiatric Research, Orangeburg, New York; and the [5]New York University School of Medicine, New York, New York.
Corresponding author: Emmanuel Planel, emmanuel@planel.org.
Received 16 February 2012 and accepted 24 July 2012.
DOI: 10.2337/db12-0187
M.-A.P. and N.B.E.K. contributed equally to this work.

Only a small proportion of AD is due to dominant genetic variants (mutations); the large majority of cases (~99%) are late-onset and sporadic in origin. The cause of sporadic AD is likely to be multifactorial, with external and biological factors interacting with genetic susceptibilities to accelerate the manifestation of the disease. Insulin dysfunction might be such a factor, as there is increasing evidence supporting a link between AD and insulin dysfunction (3). For example, compared with age-matched controls, AD brains show abnormalities in insulin and insulin receptor levels (3,4). Moreover, population-based and cohort studies have detected higher AD incidence rates in diabetic patients (5,6).

Over the last decade, there has been considerable interest on the impact of insulin dysfunction and diabetes on τ pathology. Preclinical studies have shown that insulin is capable of modulating τ phosphorylation in cultured cells (7), which was confirmed by observations of hyperphosphorylated τ in insulin knockout mice (8) or in mice with genetic impairment of insulin signaling in the brain (9). Moreover, we (10) and others (11–15) have reported τ hyperphosphorylation in mouse models of type 1 diabetes induced by intraperitoneal injection of streptozotocin (STZ).

To extend these findings, we investigated τ phosphorylation in a model that does not require drug intervention to induce type 1 diabetes, the nonobese diabetic (NOD) mice. These mice spontaneously develop type 1 diabetes at 13–25 weeks of age as a consequence of selective destruction of insulin-producing β-cells (16). Our data indicate that τ hyperphosphorylation correlated with the appearance of spontaneous diabetes in adult NOD mice, and this effect was exacerbated when the mice became hypothermic as a consequence of diabetes. Moreover, we demonstrate that this hyperphosphorylation is paralleled by a deregulation in protein phosphatase 2A (PP2A).

RESEARCH DESIGN AND METHODS

Animals. Female NOD/ShiLtJ (The Jackson Laboratory, Bar Harbor, ME) were used as the onset of type 1 diabetes symptoms occurs earlier and with a higher incidence (60–80%) in comparison with males (20–30%) (17). As these mice were originally derived from outbred Institute of Cancer Research mice (ICR, also available as CD-1 mice) (18), we used ICR (Crl:CD1 [ICR]; Charles River Laboratories, Wilmington, MA) female animals as controls. Animals were handled according to procedures approved by the Comité de Protection des Animaux under the guidelines of the Canadian Council on Animal Care.

Monitoring of physiological parameters. The diagnosis of diabetes was done by monitoring the mice for glycosuria, glycemia, and insulinemia. Mice were considered diabetic when nonfasting plasma glucose level was >12 mmol/L, and there was presence of glycosuria for 2 consecutive weeks (18). Glycosuria was monitored with reagents strips for urinalysis (Diastix; Bayer HealthCare, Pittsburgh, PA). Nonfasting blood glucose was measured using

a glucometer with reagent strips (ACCU-CHEK Aviva Nano; Roche Diagnostics, Mannheim, Germany) or a Glucose Assay Kit (Biovision Inc., Mountain View, CA). Plasma insulin was determined using a sandwich enzyme immunoassay according to the manufacturer's instructions (Mouse Insulin ELISA, Mercodia, Sweden). All mice were weighed at sacrifice, and the body temperature was monitored using a rectal probe (Thermalert TH-5; Physitemp, Clifton, NJ).

Protein extraction. Mice were killed by decapitation without anesthesia because anesthesia can increase hypothermia-induced τ phosphorylation (19). Brains were immediately removed, and tissues were dissected on ice. Cortical tissues were quickly weighed, frozen on dry ice, and maintained at −80°C. Protein extraction from frozen samples was performed as described previously (20).

Western blot analysis. SDS-PAGE and Western blot analysis was done as previously described (20). All antibodies used in this study are described in Table 1. Immunoreactive bands were visualized using the ImageQuant LAS 4000 imaging system (GE Healthcare Biosciences, Piscataway, NJ), and densitometric analysis was performed with Image Gauge analysis software (Fujifilm USA, Valhalla, NY).

Immunofluorescence. Tissue fixation was done according to the cold Bouin's method previously developed in our laboratory (21). Bound antibodies were visualized with Alexa Fluor 568–conjugated anti-mouse IgG (1:500) or Alexa Fluor 488–conjugated anti-rabbit IgG (1:1,000) (Molecular Probes, Eugene, OR). Immunolabeled tissues were observed under a Carl Zeiss Axio Imager M2 (Carl Zeiss, Jena, Germany) microscope equipped with a Nuance FX multispectral imaging system (Cambridge Research & Instrumentation, Woburn, MA) and Nuance 2.10 software (Cambridge Research & Instrumentation).

PP2A immunoprecipitation assay. Brain phosphatase activity was determined using the Ser/Thr phosphatase Assay Kit from Millipore (Temecula, CA) according to the manufacturer's instructions. After immunoprecipitation, the activity of the PP2A was assessed by the release of phosphate from a chemically synthesized phosphopeptide over a period of 10 min at 30°C. The amount of phosphate released was measured by the absorbance of the malachite green–phosphate at 630 nm.

Statistical analysis. Statistical analyses were performed with GraphPad Prism software 4.0 (GraphPad). Differences between groups were calculated for statistical significance using a one-way ANOVA followed by a Newman-Keuls post hoc test, when effects were significant ($P < 0.05$) as assessed by ANOVA: *$P < 0.05$, **$P < 0.01$, and ***$P < 0.001$ versus control. Quantitative data were presented as mean ± SD.

RESULTS

Physiological parameters of NOD and ICR mice. We separated our animals into two age groups: young (4 weeks old, $n = 5$) and adult (18–30 weeks old, $n = 18$) mice (Table 2). We followed the development of type 1 diabetes symptoms by measuring several metabolic and physiological parameters including weight, glycemia, insulinemia, glycosuria, and body temperature (Table 2), because we have previously demonstrated that alterations of glucose metabolism can induce hypothermia leading to τ hyperphosphorylation (21). At 4 weeks of age, young NOD mice were not diabetic and had lower glycemia in comparison with ICR controls, an observation that is consistent with the literature (17). No significant changes in body temperature were detected in these mice.

Adult NOD mice developed type 1 diabetes symptoms progressively and were accordingly classified into three subgroups (see Table 2 for groups and values). The first subgroup consisted of nondiabetic NOD mice ($n = 7$) with a mean age of 30 weeks. This group did not show any significant changes in blood glucose or insulin levels when compared with their ICR controls. The second group consisted of glycosuric NOD mice (NODG, $n = 7$) with a mean age of 25 weeks. These mice started to develop type 1 diabetes and were characterized by higher glycemia as well as glycosuria. Notably, blood insulin levels of this group of mice revealed hypoinsulinemia in comparison with ICR controls. Interestingly, four diabetic mice showed, in addition to hyperglycemia and glycosuria, a significant drop of body temperature, massive hyperglycemia, as well as hypoinsulinemia compared with ICR controls. Based on these observations, these mice were again classified into an NODH (NOD hypothermic and glycosuric) group ($n = 4$) with a mean age of 18 weeks (Table 2). The NODH mice were hypothermic for a maximum of 2 days before sacrifice. Thus, at the end of the study period, the incidence of diabetes was ~60% (11 out of 18 mice), which falls within the accepted incidence of diabetes in these mice (18,22). As expected, all NOD subgroups weighed significantly less than ICR control mice (Table 2). It should be noted that there are differences in age in the adult NOD group because, as we were monitoring the mice for diabetes, some of them became diabetic or hypothermic along the way and were accordingly separated in subgroups. We do not have a separate ICR control group for each age because there was no difference in τ phosphorylation between 4- and 30-week-old ICR mice (data not shown).

τ phosphorylation in young NOD mice. We first assessed whether spontaneous type 1 diabetes influences τ phosphorylation in young NOD mice by Western blot using an extensive panel of anti-τ antibodies (Table 1). At 4 weeks of age, we could not detect any significant increase in τ phosphorylation at any of the epitopes investigated in NOD mice in comparison with controls. Similarly, levels of total τ were not changed at this stage (Fig. 1).

τ phosphorylation in adult NOD mice. We next investigated τ phosphorylation in adult NOD mice. Although nondiabetic NOD mice did not show any deregulation in glucose metabolism, we observed a slight but significant increase in τ phosphorylation at pS422 (145% of control, Fig. 2*G*), which was confirmed by a significant decrease in the dephosphorylation of τ at the τ-1 epitope (82%, Fig. 2*A*). However, the appearance of distinguishing type 1 diabetes features (hyperglycemia and glycosuria) in NODG mice correlated with an extensive τ hyperphosphorylation at the AT8 (189%), CP13 (182%), pS262 (207%), and pS422 (242%) epitopes in comparison with control (100%) (Fig. 2*B*, *C*, *E*, and *G*). Interestingly, the appearance of hypothermia in the NODH group was paralleled by massive τ hyperphosphorylation at all τ-phospho–epitopes investigated (Fig. 2*B*–*G*): AT8 (1116%), CP13 (614%), TG3 (282%), pS262 (302%), PHF-1 (193%), and pS422 (508%). These results were confirmed by a significant decrease in the τ-1 epitope (83 and 60% in NODG and NODH groups, respectively; Fig. 2*A*). The pronounced hyperphosphorylation of τ in NODH mice was paralleled by a shift in the separation pattern of τ, as shown using a phospho-independent total τ antibody (Fig. 2*H*). This mobility shift reflecting τ phosphorylation was not accompanied by significant changes in the total levels of τ (Fig. 2*H*). Taken together, these results suggest that τ hyperphosphorylation at multiple epitopes follows the onset of diabetes in NOD mice and is amplified by the advent of hypothermia.

τ kinases in adult NOD mice. τ hyperphosphorylation in adult NOD mice could be attributable to either the activation of τ kinases or the inhibition of phosphatases. To discriminate between these two possibilities, we examined the activation profiles of the major τ kinases (23), including glycogen synthase kinase-3β (GSK-3β), mitogen-activated protein kinase/extracellular signal-regulated kinase (ERK), c-Jun *N*-terminal kinase (JNK), cyclin-dependent kinase 5 (cdk5), and Ca^{2+} calmodulin-dependent protein kinase (CamKII). Moreover, we studied the activation state of AKT, a key kinase implicated in the insulin-signaling pathway and also known to phosphorylate τ in vitro (24).

TABLE 1
Antibodies used in this study

Name	Abbreviation	Epitope	Type	Origin	Provider	WB	IHC
τ							
Anti–τ-1, clone PC1C6	τ-1	Non–phospho-S195, 198, 199, 202	Mono	Mouse	Millipore	1/1,000	NU
Anti–PHF-τ, clone AT8	AT8	pS202, pT205	Mono	Mouse	Thermo Scientific	1/1,000	NU
Anti–PHF-τ, clone AT100	AT100	pT212, pS214	Mono	Mouse	Thermo Scientific	1/1,000	1/500
CP13	CP13	pS202	Mono	Mouse	Peter Davies	1/1,000	NU
TG-3	TG-3	pT231	Mono	Mouse	Peter Davies	1/1,000	NU
Anti-τ (pS262)	PS262	pS262	Poly	Rabbit	Invitrogen	1/1,000	NU
PHF-1	PHF-1	pS396, pS404	Mono	Mouse	Peter Davies	1/1,000	NU
Anti-τ (pS422)	PS422	pS422	Poly	Rabbit	Invitrogen	1/1,000	NU
Anti-human τ A0024	Total τ	Human τ COOH terminus	Poly	Rabbit	Dako Cytomation	1/5,000	1/1,000
Kinases							
GSK-3β	GSK-3/-3β	Rat GSK-3β 1–160	Mono	Mouse	BD Transduction	1/1,000	NU
Phospho GSK3β (Ser9)	GSK-3/-3β S9	pS9	Poly	Rabbit	Cell Signaling Technology	1/1,000	NU
Akt	Akt	Mouse Akt COOH terminus	Poly	Rabbit	Cell Signaling Technology	1/1,000	NU
Phospho-Akt (Ser473)	P-AKT	pS473	Poly	Rabbit	Cell Signaling Technology	1/1,000	NU
p44/p42 MAPK	ERK	Rat p44 MAPK COOH terminus	Poly	Rabbit	Cell Signaling Technology	1/1,000	NU
Phospho-p44/42 MAPK (Erk1/2)	P-ERK	pT202, pY204	Poly	Rabbit	Cell Signaling Technology	1/1,000	NU
SAPK/JNK	JNK	Human JNK2	Poly	Rabbit	Cell Signaling Technology	1/1,000	NU
Phospho-SAPK/JNK	P-JNK	pT183, pY185	Poly	Rabbit	Cell Signaling Technology	1/1,000	NU
Cdk5 (C-8)	CDK5	Human cdk5 COOH terminus	Poly	Rabbit	Santa Cruz Biotechnology	1/1,000	NU
p35 (C-19)	P35	Human p35 COOH terminus	Poly	Rabbit	Santa Cruz Biotechnology	1/1,000	NU
CamKIIα (A-1)	CaMKII	Mouse CamKIIα 303–478	Mono	Mouse	Santa Cruz Biotechnology	1/1,000	NU
p-CamKIIα (Thr286)	P-CaMKII	pT286	Poly	Rabbit	Santa Cruz Biotechnology	1/1,000	NU
Phosphatases							
PP1 (E-9)	PP1	Human full-length PP1-α	Mono	Mouse	Santa Cruz Biotechnology	1/1,000	NU
Pan-calcineurin A	PP2B	Human α calcineurin A, COOH terminus	Poly	Rabbit	Cell Signaling Technology	1/1,000	NU
PP2A A subunit	PP2A A	Human PP2A A subunit (α and β)	Poly	Rabbit	Cell Signaling Technology	1/1,000	NU
Anti-PP2A, C subunit, clone 7A6	PP2A C	Human PP2A C subunit 302–309	Mono	Mouse	Millipore	1/1,000	NU
PP2A C subunit	PP2A C	Human PP2A C subunit (α and β)	Poly	Rabbit	Cell Signaling Technology	1/1,000	NU
Demethylated-PP2A-C (4B7)	PP2A C Dem	Unmethylated PP2A C COOH terminus	Mono	Mouse	Santa Cruz Biotechnology	1/1,000	NU
PPP2R2A (2G9)	PP2A Bα	Rat PPP22R2A/PP2A, B55-α/PR55-α	Mono	Mouse	Cell Signaling Technology	1/1,000	NU
PPP2R2B	PP2A Bβ	Human PPP2R2B 25–75	Poly	Rabbit	Bethyl Laboratories	1/1,000	NU
PP5	PP5	Human PP5 NH_2 terminus	Poly	Rabbit	Cell Signaling Technology	1/1,000	NU
APP/CTFs							
APP (C1/6.1)	APP/CTFs	Full-length APP and CTFs	Mono	Mouse	Paul M. Mathews	1/2,000	NU

CTF, COOH-terminal fragments; IHC, dilution used in immunohistochemistry; MAPK, mitogen-activated protein kinase; Mono, monoclonal; NU, not used; PKB, protein kinase B; Poly, polyclonal; SAPK, stress-activated protein kinase; WB, dilution used in Western blotting.

TABLE 2
Physiological parameters of ICR and NOD mice

Group	*N*	Sex	Age (weeks)	Weight (g)	Glucose (mmol/L)	Insulin (μg/L)	Glycosuria	Temperature (°C)
Young mice								
ICR	5	F	4	23.8 ± 2.5	10.1 ± 0.8	0.6 ± 0.1	−	38.0 ± 0.3
NOD	5	F	4	17.0 ± 1.2***	6.6 ± 1.3***	0.9 ± 0.3	−	38.5 ± 0.5
Adult mice								
ICR	11	F	32 ± 4	48.7 ± 7.3	7.8 ± 2.0	1.1 ± 0.6	−	37.5 ± 0.5
NOD	7	F	30 ± 4	27.2 ± 3.1***	7.9 ± 1.1	0.8 ± 0.3	−	37.9 ± 0.6
NODG	7	F	25 ± 5	24.8 ± 2.5***	12.1 ± 2.9*	0.7 ± 0.3*	+	37.3 ± 0.6
NODH	4	F	18 ± 7	18.8 ± 1.5***	25.3 ± 9.4***	0.5 ± 0.1*	+	32.7 ± 1.6***

Data are means ± SD. F, female. Asterisks indicate significant differences from controls: *$P < 0.05$, ***$P < 0.001$. Glycosuria + or − refers to the presence or absence of glucose into the urine, respectively.

We explored the activation patterns of all of these kinases with a panel of antibodies (Table 1).

The nondiabetic adult NOD mice did not show significant changes for any of the investigated kinases as compared with ICR mice (Fig. 3).

By contrast, the onset of diabetes was accompanied by several changes in the expression and activation pattern of τ kinases. Thus, both NODG and NODH mice revealed a significant increase in the phosphorylation state of GSK-3β at the Ser9 epitope, which reflects GSK-3β inhibition (Fig. 3*B*). Interestingly, we observed a strong increase in AKT phosphorylation in both diabetic NODG and NODH mice, which was accompanied by a significant decrease in the total levels of AKT (Fig. 3*C* and *D*), suggesting an activation of this kinase. However, there was no increase in τ phosphorylation in the AT100 epitope (T212/S214), a known in vitro phosphorylation site for AKT (24) at any point (data not shown).

By contrast, our data revealed a significant decrease in the levels of cdk5 and its neuronal specific activator p35 in NODG mice (Fig. 3*I* and *J*) and in the phosphorylation levels of CamKII in NODH mice (Fig. 3*L*), suggesting that the activation of these two kinases do not have a direct impact on τ phosphorylation during type 1 diabetes.

Therefore, AKT was the only kinase activated in adult NOD mice, but this activation failed to explain the extent of τ hyperphosphorylation, especially at epitopes not phosphorylated by AKT. Thus, kinase activation was probably not the primary mechanism leading to τ hyperphosphorylation in type 1 diabetes.

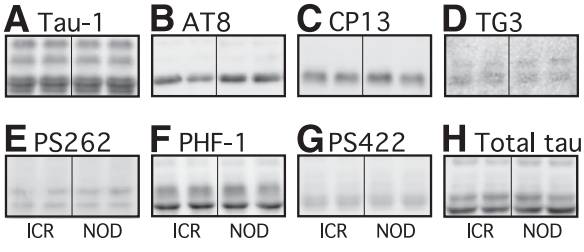

FIG. 1. Effect of type 1 diabetes on τ phosphorylation in young NOD mice. Proteins from 4-week-old mice were extracted from mice cortices, separated by SDS-PAGE, and identified with the following antibodies: *A*: Tau-1; *B*: AT8; *C*: CP13; *D*: TG3; *E*: PS262; *F*: PHF-1; *G*: PS422; and *H*: total τ. Lanes are identified as follows: *lanes 1* & *2*, young ICR control mice; *lanes 3* & *4*, young NOD mice. For each epitope, two representative lanes from each group are displayed. Dividing lines represent areas where lanes were removed and the remaining lanes were spliced together.

τ phosphatases in adult NOD mice. As our results failed to adequately explain the extent of τ hyperphosphorylation specific to type 1 diabetes in terms of kinase activation, we next assessed the expression levels of τ Ser/Thr protein phosphatases (PP). PP are classified into five types: PP1, PP2A, PP2B, PP2C, and PP5, all of them being highly expressed in the mammalian brain (25). Biochemical studies have previously demonstrated that all PP except PP2C can dephosphorylate τ in vitro (26). We thus examined the profiles of these four PP using specific antibodies (Table 1).

As shown in Fig. 4*A*, levels of PP1 did not significantly change in all groups tested. By contrast, PP2B showed a significant decrease in both nondiabetic NOD and glycosuric NODG mice (Fig. 4*B*). In addition, we observed a slight increase in the expression of PP5 in NODH mice (Fig. 4*H*).

PP2A is a heterotrimeric holoenzyme consisting of a core dimer composed of a catalytic subunit (C) tightly bound with the scaffolding (A) subunit, and this core dimer associates with a variable regulatory B subunit. Only trimeric forms of PP2A containing the Bα or Bβ subunits associate with neural microtubules (27). Moreover, PP2A activity is enhanced by the methylation of its catalytic subunit (PP2A C) and is conversely decreased by its demethylation (28).

Thus, we investigated levels of PP 2A, A scaffolding subunit (PP2A A), PP2A C, PP2A C Dem (demethylated, inactivated), PP2A B regulatory subunit, α isoform (PP2A Bα), and PP2A B regulatory subunit, β isoform (PP2A Bβ) subunits in adult NOD mice. Whereas the expression of the PP2A A scaffolding subunit was mildly decreased only in the group of NODG mice (Fig. 4*C*), the PP2A C catalytic subunit was significantly increased in both NODG and NODH groups in comparison with controls (Fig. 4*D*). Accordingly, immunoblots revealed an increase of the demethylated form of PP2AC in both NODG and NODH mice (Fig. 4*E*). The PP2A Bα subunit was significantly downregulated in all NOD groups, whereas PP2A Bβ expression was decreased only in nondiabetic NOD mice (Fig. 4*F* and *G*). In addition, we observed a significant decrease in brain PP2A activity in NODG and NODH mice (Fig. 4*I*).

Overall, the most notable changes in phosphatases in adult NOD mice were in the subunits of PP2A, including an increase in the total level of PP2A C and the demethylation of PP2A C (i.e., inhibition of the activity of the catalytic subunit), a decrease in the levels of PP2A Bα, and an inhibition of PP2A enzymatic activity. These results demonstrate a deregulation of PP2A in NODG and NODH mice compared with ICR controls.

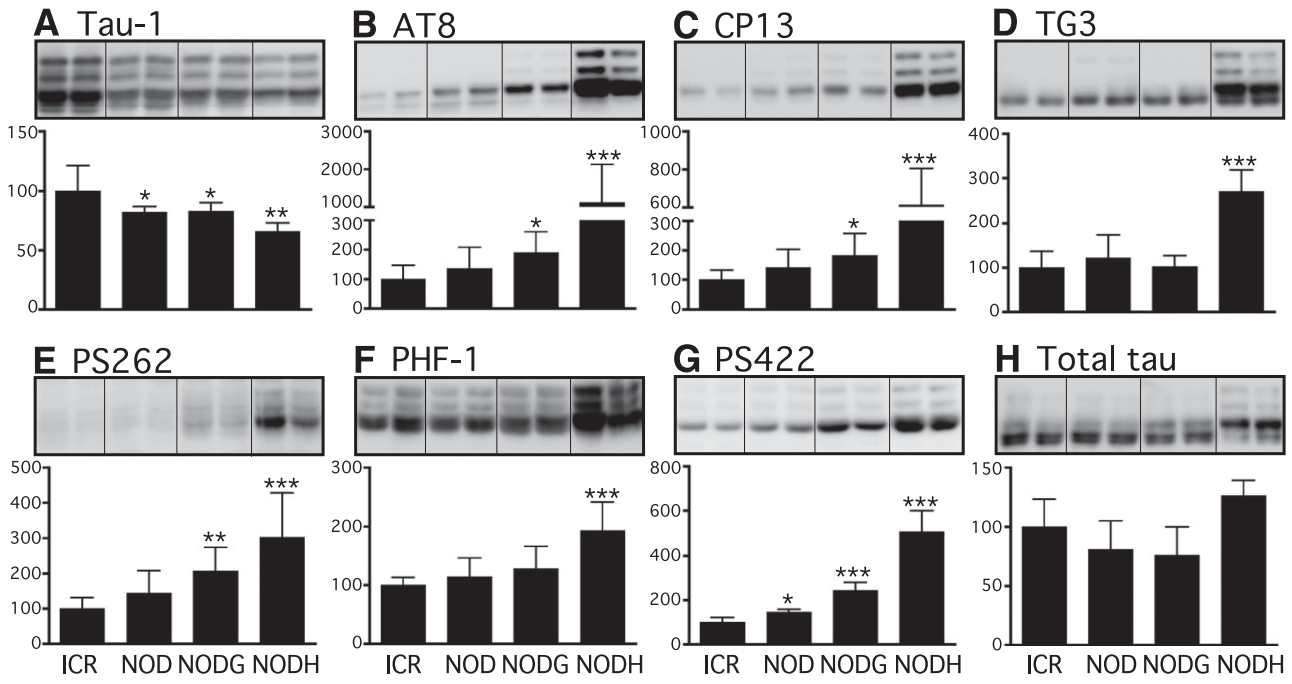

FIG. 2. Effect of type 1 diabetes on τ phosphorylation in adult NOD mice. Proteins from mice 18 to 30 weeks of age were extracted from mice cortices, separated by SDS-PAGE, and identified with the following antibodies: *A*: Tau-1, *B*: AT8, *C*: CP13, *D*: TG3, *E*: PS262, *F*: PHF-1, *G*: PS422, and *H*: total τ. Lanes are identified as follows: *lanes 1* & *2*, ICR control mice; *lanes 3* & *4*, nondiabetic NOD mice; *lanes 5* & *6*, diabetic glycosuric NODG mice, and *lanes 7* & *8*, glycosuric and hypothermic NODH mice. For each epitope, two representative lanes from each group are displayed. Dividing lines represent areas where lanes were removed and the remaining lanes were spliced together. Data are means ± SD. Asterisks indicate significant differences from controls, with *$P < 0.05$, **$P < 0.01$, and ***$P < 0.001$.

Regional analysis of τ hyperphosphorylation. In AD, the earliest detectable τ hyperphosphorylation is localized in neurites of vulnerable neurons before undergoing somatodendritic relocalization (29) and aggregation as NFTs (30). To investigate a possible relocalization of τ and further validate our immunoblot experiments, we examined the gross anatomical pattern of τ phosphorylation by immunofluorescence. Staining of hippocampal sagittal sections clearly showed a robust increase in phospho-τ immunoreactivity at the AT8 epitope in NODH mice and to a much lesser extent in the NODG group in comparison with ICR controls (Fig. 5*A*–*C*). However, we did not detect significant changes in total or phospho-τ cellular localization, as revealed by AT8, total τ, and DAPI staining patterns (Fig. 5*D*–*I*).

Amyloid precursor protein metabolism in NOD mice. We also wanted to address the possibility that changes in amyloid precursor protein (APP) metabolism could be a plausible driving force for altered τ phosphorylation in NOD mice (31). Except for a mild decrease in APP full-length in nondiabetic NOD mice, no other significant changes were observed in either APP full-length or APP COOH-terminal fragment levels in adult NOD mice (data not shown). These results confirm our previous data demonstrating that APP metabolism is not affected in mice with STZ-induced type 1 diabetes (10) and suggest that τ hyperphosphorylation in NOD mice is not the result of alterations in APP metabolism.

DISCUSSION

In this study, we investigated τ phosphorylation and its molecular mechanisms in the NOD mouse strain, one of the most valuable genetic animal models for type 1 diabetes (32). Our data suggest that spontaneous type 1 diabetes provokes a progressive τ hyperphosphorylation that begins to be detectable in adult mice even during the nondiabetic stage, in which there is no apparent deregulation of glucose metabolism. We further show that τ phosphorylation is greatly exacerbated in the presence of principal type 1 diabetes features, notably hyperglycemia and glycosuria, and further amplified by hypothermia. Finally, we demonstrate that τ hyperphosphorylation during type 1 diabetes is likely attributable to a deregulation in PP2A, the major τ phosphatase in vivo.

Our findings are consistent with our previous study (10) and several other studies showing τ hyperphosphorylation at several epitopes in type 1 diabetes induced by STZ in mice (11–13), or rats (14). However, many of these articles did not document the temperature of the animals. This is important because we have reported before (10), and confirmed in this study, that τ phosphorylation is increased when diabetic mice become hypothermic. Indeed, decreased temperature is a common outcome in both human (33) and experimental diabetes (10,34), and hypothermia is a powerful regulator of τ phosphorylation, increasing it by 80% per degree Celsius below 37°C in mice (21).

In comparison with our previous study in STZ-treated mice (10), several differences can be noted in the pattern of τ phosphorylation with the NOD mice. For example, in this study we observed that the AT8, pS262, and pS422 epitopes were hyperphosphorylated in nonhypothermic NODG mice, whereas these epitopes did not show any significant changes in the absence of hypothermia in STZ-induced animals. In contrast, τ phosphorylation at the PHF-1 epitope was increased only in the group of hypothermic NODH mice, whereas we have detected a significant increase in this epitope in nonhypothermic mice

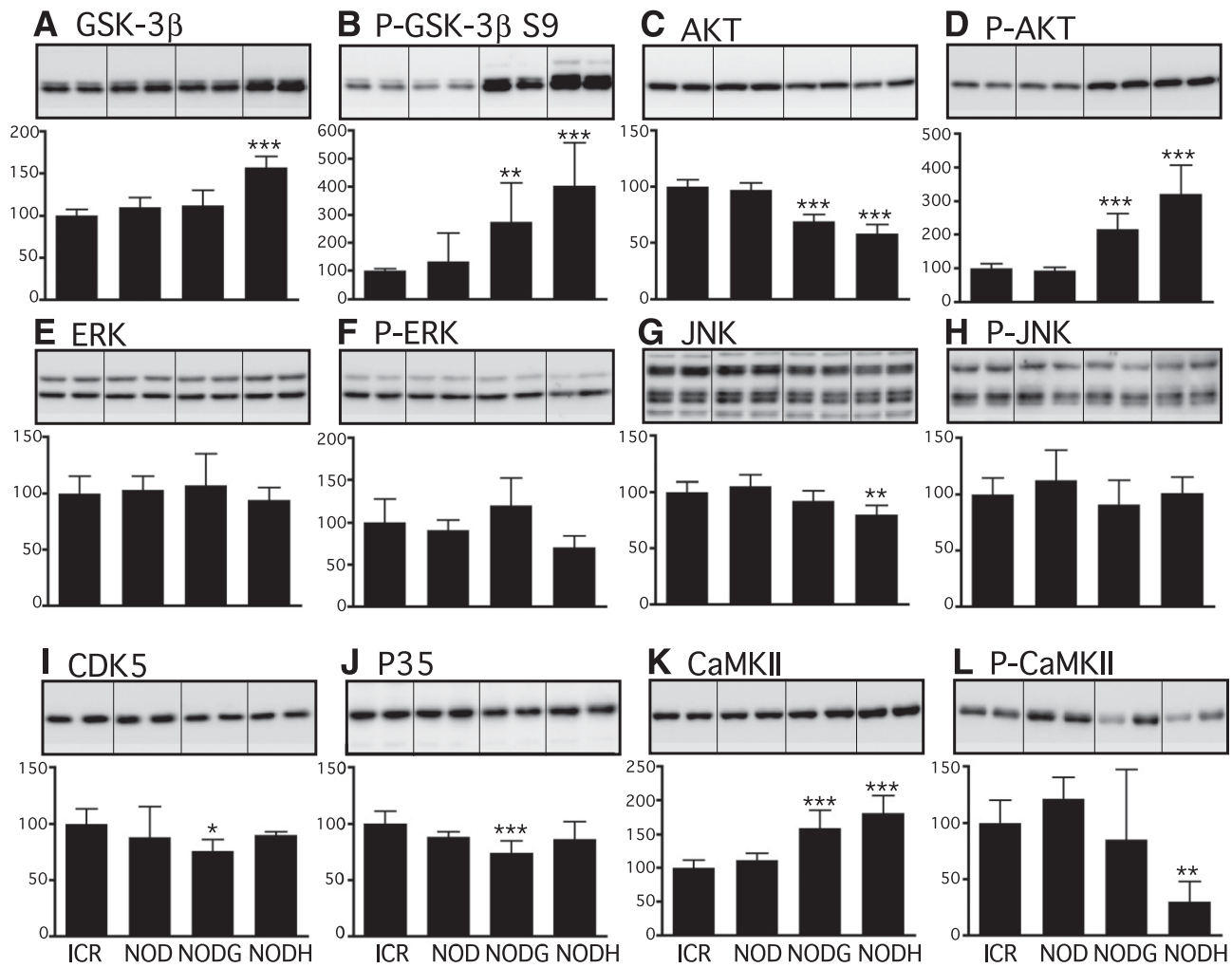

FIG. 3. Effect of type 1 diabetes on τ kinases in adult NOD mice. Proteins from mice 18 to 30 weeks of age were extracted from mice cortices, separated by SDS-PAGE, and identified with the following antibodies: *A*: GSK-3β, *B*: pGSK-3β S9, *C*: AKT, *D*: P-AKT, *E*: ERK, *F*: P-ERK, *G*: JNK, *H*: P-JNK, *I*: CDK5, *J*: P35, *K*: CamKII, and *L*: P-CamKII. Lanes are identified as follows: *lanes 1* & *2*, ICR control mice; *lanes 3* & *4*, nondiabetic NOD mice; *lanes 5* & *6*, diabetic glycosuric NODG mice, and *lanes 7* & *8*, glycosuric and hypothermic NODH mice. For each epitope, two representative lanes from each group are displayed. Dividing lines represent areas where lanes were removed and the remaining lanes were spliced together. Data are means ± SD. Asterisks indicate significant differences from controls, with *$P < 0.05$, **$P < 0.01$, and ***$P < 0.001$.

following STZ treatment (10). These differences could be due to the fact that NOD and STZ-induced mice develop insulin deficiency that characterizes type 1 diabetes in a differential manner. Indeed, whereas NOD mice showed lower (but detectable) blood insulin levels in comparison with control, insulin levels were not detectable in STZ-induced animals (10). Another possible explanation is that STZ might have a direct impact on τ phosphorylation in the brain. Although peripheral administration of STZ is not thought to impact the brain directly because its transport and cytotoxicity are dependent on the GLUT-2 glucose transporter (35), GLUT-2 has also been found in the mammalian brain, and intracerebroventricular application of STZ in minute amounts has been reported to directly induce τ hyperphosphorylation (36). Thus, NOD mice might be models more relevant to humans to study the impact of insulin dysfunction on τ phosphorylation during diabetes.

We observed τ hyperphosphorylation at the pS422 epitope in nondiabetic NOD mice prior to deregulation in the glucose metabolism. This epitope is associated with early pretangle formation (37) and the promotion of τ aggregation (38) and is characteristic of abnormal AD-like τ phosphorylation. Concurrent with hyperglycemia and glycosuria in adult NOD mice, τ phosphorylation increased at additional epitopes, notably AT8, CP13, pS262, PHF-1, and pS422. Some of these sites have been linked to specific aspects of τ pathology such as the inhibition of τ microtubules binding (e.g., Ser262) (39) and the promotion of τ aggregation (e.g., Ser396 and Ser422) (38). Moreover, PHF-1 is associated with late-paired helical filament and NFT formation (40). Therefore, it appears that insulin dysfunction results in an increase in τ phosphorylation at epitopes that are critical for the development of τ pathology.

During the nondiabetic stage, adult NOD mice did not show any changes in expression and activation patterns of all investigated kinases. We observed an increase in inhibitory phosphorylation of GSK-3β in both NODG and NODH mice, in accordance with previous studies revealing inhibition of GSK-3β in STZ-induced animal models (10,11,41). However, it should be mentioned that the elevation of GSK-3β Ser9 in NODH mice is not surprising, because GSK-3β Ser9 phosphorylation is a constant result of hypothermia in the mouse brain (21). The increased

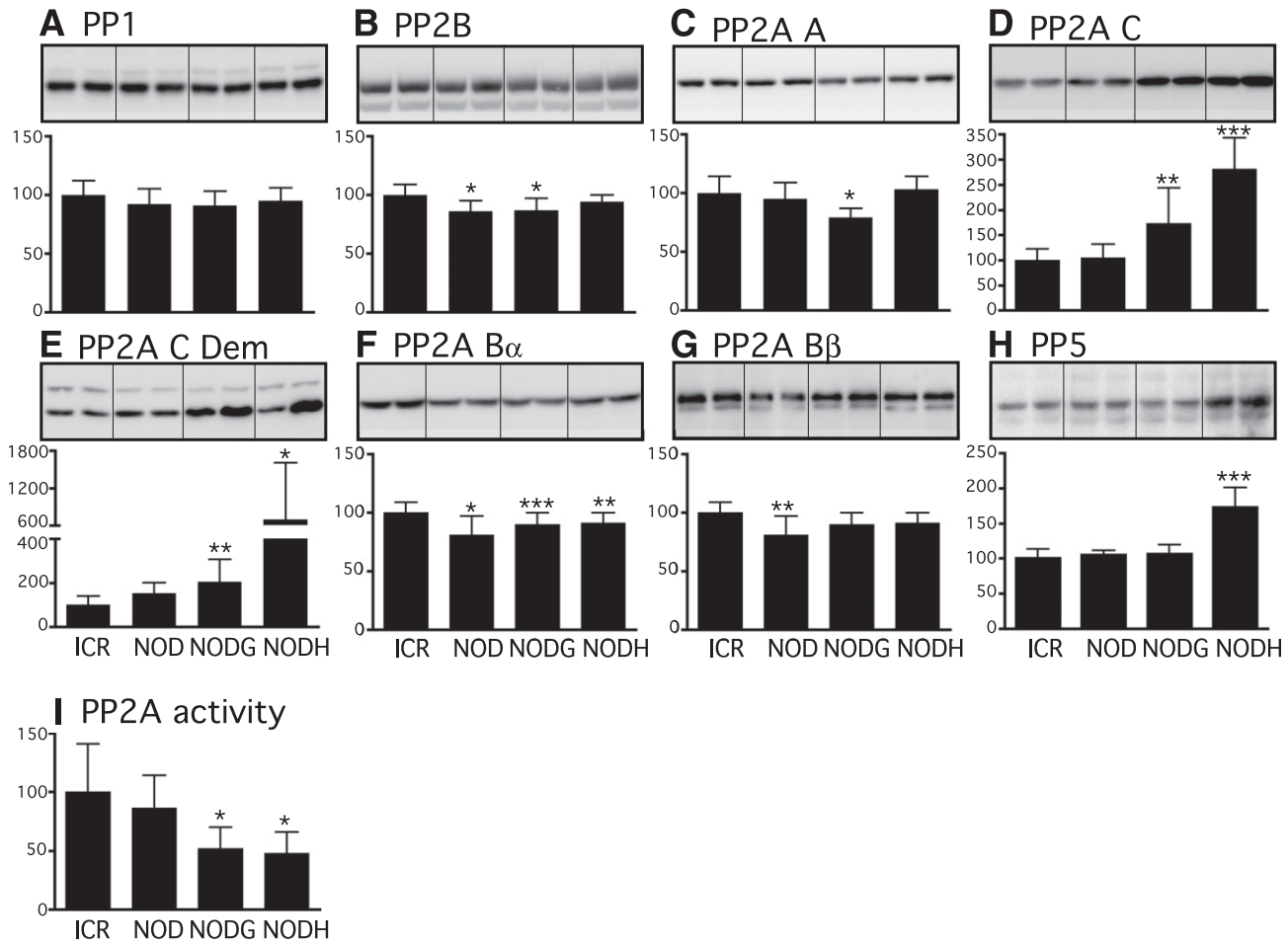

FIG. 4. Effect of type 1 diabetes on τ phosphatases in adult NOD mice. Proteins from mice 18 to 30 weeks of age were extracted from mice cortices, separated by SDS-PAGE, and identified with the following antibodies: *A*: PP1, *B*: PP2B, *C*: PP2A A, *D*: PP2A C, *E*: Demethylated PP2A C (PP2A C Dem), *F*: PP2A Bα, *G*: PP2A Bβ, *H*: PP5, and *I*: PP2A activity. Lanes are identified as follows: *lanes 1* & *2*, ICR control mice; *lanes 3* & *4*, nondiabetic NOD mice; *lanes 5* & *6*, diabetic glycosuric NODG mice, and *lanes 7* & *8*, glycosuric and hypothermic NODH mice. For each epitope, two representative lanes from each group are displayed. Dividing lines represent areas where lanes were removed and the remaining lanes were spliced together. Data are means ± SD. Asterisks indicate significant differences from controls, with *$P < 0.05$, **$P < 0.01$, and ***$P < 0.001$.

phosphorylation of Ser9 could be explained by the activation of AKT observed in NODG and NODH mice. In fact, AKT was the only kinase activated in NOD mice, and its activation failed to explain the extent of τ hyperphosphorylation at multiple epitopes.

The analysis of different τ phosphatases in type 1 diabetes animal models is less documented compared with kinases. However, we (10) and others (11,14) have reported that PP2A is inhibited in STZ-induced animal models. In this study, we detected a decrease in the Bα regulatory subunit and an increase in demethylated (inhibition) and total PP2A catalytic subunit in NODG and NODH mice. These changes were paralleled by a significant decrease in the activity of PP2A. Although seemingly counterintuitive, the increase of the catalytic subunit along with a decrease in activity can be explained by the potent autoregulatory mechanism that adjusts PP2A C levels according to PP2A activity, in which inhibition of PP2A leads to the accumulation of the C subunit, either in vitro or in vivo (20,42). These results corroborate our previous observation of increased PP2A C concomitant with decreased PP2A activity in STZ-treated mice (10).

We also observed changes in PP2B and PP5 levels, but among all phosphatases that dephosphorylate τ, PP2A is the major τ phosphatase in vivo, with PP2A, PP1, PP5, and PP2B contributing to 71, 11, 10, and 7%, respectively, of the total τ phosphatase activity in the brain (43).

Importantly, PP2A can regulate the phosphorylation of all the sites studied in this paper (43), and its deregulation is thought to be an important factor in the evolution of AD pathology (26). Taken together, our results suggest that the progressive deregulation of PP2A in NOD mice is likely to be the cause of the observed τ hyperphosphorylation.

An important question is whether it is peripheral and/or central insulin dysfunction that causes PP2A deregulation and τ hyperphosphorylation. Some studies may hint that central insulin dysfunction is not involved in the phenotype of the NOD mice. For example, central insulin dysfunction, whether it is in patients (44) or mediated by knocking out the brain insulin receptor (9) or by direct injections of STZ in the rodent brain (36,45), does correlate with increased τ phosphorylation, but also with decreased AKT and GSK-3β Ser9 phosphorylation, the reverse of what we observed in NOD mice. In contrast, mice treated with STZ peripherally mirror what we observed in NOD mice, namely inhibition of PP2A and augmented phosphorylation of τ, AKT, and GSK-3β (10,11,46). It is interesting to note that the rise in AKT and GSK-3β Ser9

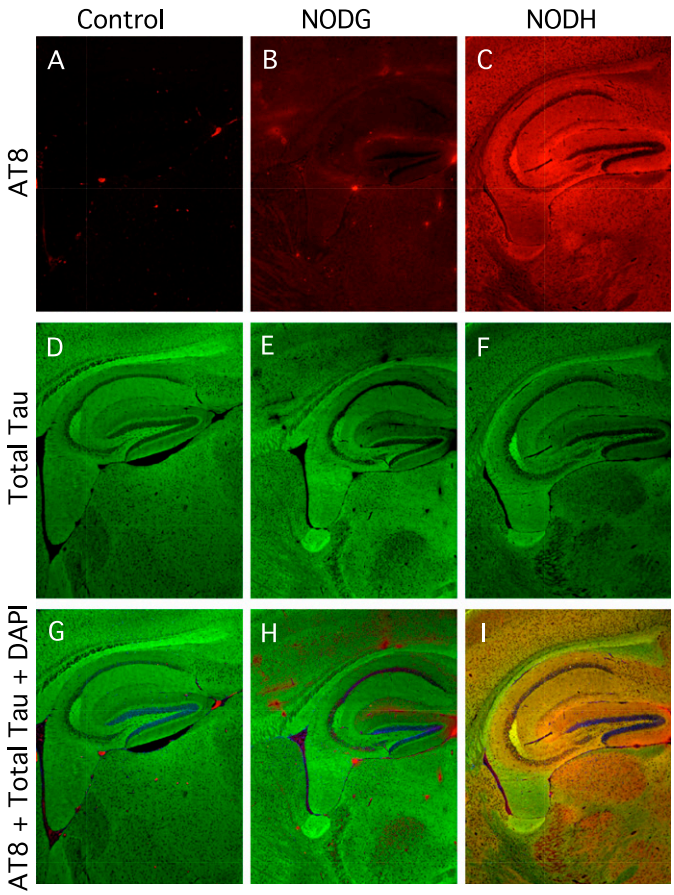

FIG. 5. Regional anatomical localization of phosphorylated τ protein in adult NOD mice. Unmixed fluorescent photomicrographs of hippocampal sagittal sections are shown with AT8 (Red, *A–C*), Total Tau (Green, *D–F*), or merged with DAPI (*G–I*), for the following conditions: control (ICR mice, *A,D,G*), glycosuric NODG mice (*B,E,H*), or glycosuric and hypothermic NODH mice (*C,F,I*). All images were taken at original magnification ×5.

phosphorylation in both NOD and STZ-treated mice is probably due to the inhibition of PP2A, as inhibitors of the phosphatase upregulate the phosphorylation of the two kinases (20,47). However, how peripheral insulin dysfunction results in central PP2A inhibition remains to be elucidated.

It is now believed that diabetes is associated with higher risk of AD pathogenesis (48). Many longitudinal population-based studies have detected lower cognitive performance in type 1 diabetes patients and higher AD incidence rates in type 2 diabetes patients (5,6,48). Type 2 diabetes, the most common form of diabetes, is preceded in most individuals by insulin resistance and hyperinsulinemia to maintain glucose homeostasis (49). However, over time, the pancreas becomes unable to produce enough insulin and β-cells burn out, leading to a dramatic decrease in insulin production, causing full-blown diabetes (50). Thus, although NOD mice do not represent a model of early type 2 diabetes, it is still valuable to address the mechanisms related to the low insulin levels that accompany type 2 diabetes in the end of its natural history.

In summary, we demonstrated that in NOD mice, the induction of diabetes leads to a progressive AD-like τ hyperphosphorylation likely due to a deregulation of the PP2A complex. Our results suggest that the NOD mice are probably one of the most valuable and relevant models to study the effects of insulin dysfunction on τ phosphorylation in the brain. Crossing NOD mice with mouse models that express human τ and develop NFTs might further help us to understand the impact of diabetes on the pathogenesis of AD.

ACKNOWLEDGMENTS

This work was supported by a Biomedical Doctoral Award from the Alzheimer Society of Canada (to N.B.E.K.), Postdoctoral Awards from the Alzheimer Society of Canada and the Alzheimer Society of Saskatchewan (to C.J.), and grants to E.P. from the Canadian Institutes of Health Research (MOP-106423 and PCN-102993), Fonds de Recherche en Santé du Québec (16205 and 20048), and the Natural Sciences and Engineering Research Council of Canada (354722). The funders had no role in study design, data collection, and analysis, decision to publish, or preparation of this manuscript.

No potential conflicts of interest relevant to this article were reported.

M.-A.P. and N.B.E.K. performed the experiments and wrote the manuscript. F.Ma., C.J., F.Mo., A.B., and F.R.P. performed the experiments. S.G., A.A., and P.M.M. contributed to the RESEARCH DESIGN AND METHODS and the DISCUSSION sections and reviewed the manuscript. S.S.H. contributed to the discussion and reviewed the manuscript. E.P. designed the experiments and wrote the manuscript. E.P. is the guarantor of this work and, as such, had full access to all the data in the study and takes responsibility for the integrity of the data and the accuracy of the data analysis.

The authors thank Dr. Peter Davies (Albert Einstein University, New York, NY) for the generous gift of τ antibodies.

REFERENCES

1. Alonso AC, Zaidi T, Novak M, Grundke-Iqbal I, Iqbal K. Hyperphosphorylation induces self-assembly of tau into tangles of paired helical filaments/straight filaments. Proc Natl Acad Sci USA 2001;98:6923–6928
2. Bretteville A, Planel E. Tau aggregates: toxic, inert, or protective species? J Alzheimers Dis 2008;14:431–436
3. Craft S, Watson GS. Insulin and neurodegenerative disease: shared and specific mechanisms. Lancet Neurol 2004;3:169–178
4. Frölich L, Blum-Degen D, Riederer P, Hoyer S. A disturbance in the neuronal insulin receptor signal transduction in sporadic Alzheimer's disease. Ann N Y Acad Sci 1999;893:290–293
5. Leibson CL, Rocca WA, Hanson VA, et al. Risk of dementia among persons with diabetes mellitus: a population-based cohort study. Am J Epidemiol 1997;145:301–308
6. Ott A, Stolk RP, van Harskamp F, Pols HA, Hofman A, Breteler MM. Diabetes mellitus and the risk of dementia: The Rotterdam Study. Neurology 1999;53:1937–1942
7. Lesort M, Jope RS, Johnson GV. Insulin transiently increases tau phosphorylation: involvement of glycogen synthase kinase-3beta and Fyn tyrosine kinase. J Neurochem 1999;72:576–584
8. Schechter R, Beju D, Miller KE. The effect of insulin deficiency on tau and neurofilament in the insulin knockout mouse. Biochem Biophys Res Commun 2005;334:979–986
9. Schubert M, Gautam D, Surjo D, et al. Role for neuronal insulin resistance in neurodegenerative diseases. Proc Natl Acad Sci USA 2004;101:3100–3105
10. Planel E, Tatebayashi Y, Miyasaka T, et al. Insulin dysfunction induces in vivo tau hyperphosphorylation through distinct mechanisms. J Neurosci 2007;27:13635–13648
11. Clodfelder-Miller BJ, Zmijewska AA, Johnson GV, Jope RS. Tau is hyperphosphorylated at multiple sites in mouse brain in vivo after streptozotocin-induced insulin deficiency. Diabetes 2006;55:3320–3325

12. Jolivalt CG, Lee CA, Beiswenger KK, et al. Defective insulin signaling pathway and increased glycogen synthase kinase-3 activity in the brain of diabetic mice: parallels with Alzheimer's disease and correction by insulin. J Neurosci Res 2008;86:3265–3274
13. Kim B, Backus C, Oh S, Hayes JM, Feldman EL. Increased tau phosphorylation and cleavage in mouse models of type 1 and type 2 diabetes. Endocrinology 2009;150:5294–5301
14. Qu Z, Jiao Z, Sun X, Zhao Y, Ren J, Xu G. Effects of streptozotocin-induced diabetes on tau phosphorylation in the rat brain. Brain Res 2011;1383:300–306
15. Ke YD, Delerue F, Gladbach A, Götz J, Ittner LM. Experimental diabetes mellitus exacerbates tau pathology in a transgenic mouse model of Alzheimer's disease. PLoS ONE 2009;4:e7917
16. Makino S, Kunimoto K, Muraoka Y, Mizushima Y, Katagiri K, Tochino Y. Breeding of a non-obese, diabetic strain of mice. Jikken Dobutsu 1980;29:1–13
17. Amrani A, Durant S, Throsby M, Coulaud J, Dardenne M, Homo-Delarche F. Glucose homeostasis in the nonobese diabetic mouse at the prediabetic stage. Endocrinology 1998;139:1115–1124
18. Leiter EH. The NOD mouse: a model for insulin-dependent diabetes mellitus. Curr Protoc Immunol 2001;Chapter 15:Unit 15.19
19. Planel E, Richter KE, Nolan CE, et al. Anesthesia leads to tau hyperphosphorylation through inhibition of phosphatase activity by hypothermia. J Neurosci 2007;27:3090–3097
20. Planel E, Yasutake K, Fujita SC, Ishiguro K. Inhibition of protein phosphatase 2A overrides tau protein kinase I/glycogen synthase kinase 3 beta and cyclin-dependent kinase 5 inhibition and results in tau hyperphosphorylation in the hippocampus of starved mouse. J Biol Chem 2001;276:34298–34306
21. Planel E, Miyasaka T, Launey T, et al. Alterations in glucose metabolism induce hypothermia leading to tau hyperphosphorylation through differential inhibition of kinase and phosphatase activities: implications for Alzheimer's disease. J Neurosci 2004;24:2401–2411
22. Olivieri A, De Angelis S, Dionisi S, et al. Serum transforming growth factor β1 during diabetes development in non-obese diabetic mice and humans. Clin Exp Immunol 2010;162:407–414
23. Planel E, Sun X, Takashima A. Role of GSK-3 beta in Alzheimer's disease pathology. Drug Dev Res 2002;56:491–510
24. Ksiezak-Reding H, Pyo HK, Feinstein B, Pasinetti GM. Akt/PKB kinase phosphorylates separately Thr212 and Ser214 of tau protein in vitro. Biochim Biophys Acta 2003;1639:159–168
25. Cohen P. The structure and regulation of protein phosphatases. Annu Rev Biochem 1989;58:453–508
26. Tian Q, Wang J. Role of serine/threonine protein phosphatase in Alzheimer's disease. Neurosignals 2002;11:262–269
27. Price NE, Wadzinski B, Mumby MC. An anchoring factor targets protein phosphatase 2A to brain microtubules. Brain Res Mol Brain Res 1999;73:68–77
28. Janssens V, Goris J. Protein phosphatase 2A: a highly regulated family of serine/threonine phosphatases implicated in cell growth and signalling. Biochem J 2001;353:417–439
29. Su JH, Cummings BJ, Cotman CW. Early phosphorylation of tau in Alzheimer's disease occurs at Ser-202 and is preferentially located within neurites. Neuroreport 1994;5:2358–2362
30. Braak E, Braak H, Mandelkow EM. A sequence of cytoskeleton changes related to the formation of neurofibrillary tangles and neuropil threads. Acta Neuropathol 1994;87:554–567
31. Gasparini L, Netzer WJ, Greengard P, Xu H. Does insulin dysfunction play a role in Alzheimer's disease? Trends Pharmacol Sci 2002;23:288–293
32. Kikutani H, Makino S. The murine autoimmune diabetes model: NOD and related strains. Adv Immunol 1992;51:285–322
33. Neil HA, Dawson JA, Baker JE. Risk of hypothermia in elderly patients with diabetes. Br Med J (Clin Res Ed) 1986;293:416–418
34. Kilgour RD, Williams PA. Effects of diabetes and food deprivation on shivering activity during progressive hypothermia in the rat. Comp Biochem Physiol A Physiol 1996;114:159–165
35. Schnedl WJ, Ferber S, Johnson JH, Newgard CB. STZ transport and cytotoxicity. Specific enhancement in GLUT2-expressing cells. Diabetes 1994;43:1326–1333
36. Grünblatt E, Salkovic-Petrisic M, Osmanovic J, Riederer P, Hoyer S. Brain insulin system dysfunction in streptozotocin intracerebroventricularly treated rats generates hyperphosphorylated tau protein. J Neurochem 2007;101:757–770
37. Augustinack JC, Schneider A, Mandelkow E-M, Hyman BT. Specific tau phosphorylation sites correlate with severity of neuronal cytopathology in Alzheimer's disease. Acta Neuropathol 2002;103:26–35
38. Gong CX, Iqbal K. Hyperphosphorylation of microtubule-associated protein tau: a promising therapeutic target for Alzheimer disease. Curr Med Chem 2008;15:2321–2328
39. Drewes G, Trinczek B, Illenberger S, et al. Microtubule-associated protein/microtubule affinity-regulating kinase (p110mark). A novel protein kinase that regulates tau-microtubule interactions and dynamic instability by phosphorylation at the Alzheimer-specific site serine 262. J Biol Chem 1995;270:7679–7688
40. Goedert M, Jakes R, Crowther RA, et al. Epitope mapping of monoclonal antibodies to the paired helical filaments of Alzheimer's disease: identification of phosphorylation sites in tau protein. Biochem J 1994;301:871–877
41. Li ZG, Zhang W, Sima AA. Alzheimer-like changes in rat models of spontaneous diabetes. Diabetes 2007;56:1817–1824
42. Baharians Z, Schönthal AH. Autoregulation of protein phosphatase type 2A expression. J Biol Chem 1998;273:19019–19024
43. Liu F, Grundke-Iqbal I, Iqbal K, Gong CX. Contributions of protein phosphatases PP1, PP2A, PP2B and PP5 to the regulation of tau phosphorylation. Eur J Neurosci 2005;22:1942–1950
44. Liu Y, Liu F, Grundke-Iqbal I, Iqbal K, Gong CX. Deficient brain insulin signalling pathway in Alzheimer's disease and diabetes. J Pathol 2011;225:54–62
45. Plaschke K, Kopitz J, Siegelin M, et al. Insulin-resistant brain state after intracerebroventricular streptozotocin injection exacerbates Alzheimer-like changes in Tg2576 AbetaPP-overexpressing mice. J Alzheimers Dis 2010;19:691–704
46. Clodfelder-Miller B, De Sarno P, Zmijewska AA, Song L, Jope RS. Physiological and pathological changes in glucose regulate brain Akt and glycogen synthase kinase-3. J Biol Chem 2005;280:39723–39731
47. Andjelković M, Jakubowicz T, Cron P, Ming XF, Han JW, Hemmings BA. Activation and phosphorylation of a pleckstrin homology domain containing protein kinase (RAC-PK/PKB) promoted by serum and protein phosphatase inhibitors. Proc Natl Acad Sci USA 1996;93:5699–5704
48. Sims-Robinson C, Kim B, Rosko A, Feldman EL. How does diabetes accelerate Alzheimer disease pathology? Nat Rev Neurol 2010;6:551–559
49. Festa A, Williams K, D'Agostino R Jr, Wagenknecht LE, Haffner SM. The natural course of beta-cell function in nondiabetic and diabetic individuals: the Insulin Resistance Atherosclerosis Study. Diabetes 2006;55:1114–1120
50. DeFronzo RA. Pathogenesis of type 2 diabetes mellitus. Med Clin North Am 2004;88:787–835